



LJMU Research Online

Guo, J, Liao, B, Liu, L, Gao, Y, Ren, X and Yang, Q

Composition Optimization and Experimental Characterization of a Novel Steel Based on CALPHAD

<http://researchonline.ljmu.ac.uk/id/eprint/3737/>

Article

Citation (please note it is advisable to refer to the publisher's version if you intend to cite from this work)

Guo, J, Liao, B, Liu, L, Gao, Y, Ren, X and Yang, Q (2015) Composition Optimization and Experimental Characterization of a Novel Steel Based on CALPHAD. JOURNAL OF MATERIALS ENGINEERING AND PERFORMANCE, 24 (5). pp. 2099-2107. ISSN 1059-9495

LJMU has developed **LJMU Research Online** for users to access the research output of the University more effectively. Copyright © and Moral Rights for the papers on this site are retained by the individual authors and/or other copyright owners. Users may download and/or print one copy of any article(s) in LJMU Research Online to facilitate their private study or for non-commercial research. You may not engage in further distribution of the material or use it for any profit-making activities or any commercial gain.

The version presented here may differ from the published version or from the version of the record. Please see the repository URL above for details on accessing the published version and note that access may require a subscription.

For more information please contact researchonline@ljmu.ac.uk

<http://researchonline.ljmu.ac.uk/>

Composition optimization and experimental characterization of a novel steel based on CALPHAD

Jing Guo^a, Bo Liao^a, Ligang Liu^a, Yukui Gao^b, Xuejun Ren^c, and Qingxiang Yang^{a,}*

^a State Key Laboratory of Metastable Materials Science & Technology, Yanshan University, Qinhuangdao 066004, China

^b Institute of Aeronautical Materials, Beijing 100095, China

^c School of Engineering, Liverpool John Moores University, Liverpool L3 3AF, UK

*Corresponding author: Tel. +86-335-838-7471 Fax. +86-335-807-4545

E-mail address: qxyang@ysu.edu.cn, guojing@ysu.edu.cn

A new steel with high Cr and low W, Mo contents for forged cold work roll was designed based on the composition system of traditional high speed steel (HSS) roll. The Fe-C isopleths of the steel and the mass fraction of equilibrium phases versus temperature were calculated by Thermo-Calc, and the effects of different alloying elements (W, Mo, Cr, V) on austenite, ferrite and carbides (MC , M_6C , M_7C_3 , $M_{23}C_6$) were also established to optimize the composition and structure. The designed and optimized specimens were both quenched at 1100°C and then tempered twice at 560°C. The hardness and wear resistance of the samples were measured. The microstructures of quenched tempered and forged specimens were studied. The results show that ferrite crystallization, peritectic reaction, austenite crystallization and the precipitation of MC , M_6C , M_7C_3 , $M_{23}C_6$ occur during equilibrium solidification process. The alloying elements W, Mo mainly affect the precipitation of M_6C , while Cr affects the precipitated region and mass fraction of M_7C_3 . High V content widens the high temperature region of the peritectic reaction and results in a large amount of MC precipitates. The optimized composition (wt%) for cold work roll steel is 1.30-1.35%C, 9-10%Cr, 2.5-3.0%Mo, 0.5-1.0%W, 2.5-3.0%V, 0.5-0.6%Mn, 0.5-0.6%Si. The hardness of the steel after quenching and tempering is 60.8HRC and weight loss after 120min is 6.2mg. This meets the requirement of hardness and wear resistance requirements for cold work roll. The ledeburite in the optimized steel disappears after forging and the carbide network break into a large amount of tiny blocky ones dispersed in the matrix without cracks, which shows a good forgeability of the steel and rationality of the optimized composition.

Keywords: carbon/alloy steels; forging; modeling processes; heat treating

1. Introduction

Cold work roll is the main tool to produce/manufacture steel strip and sheets. It is produced through a complicated manufacturing technology with much better overall quality than roll made through other production route (Ref 1). The roll is required to have a high hardness (more than 60 HRC), wear resistance, good stripping resistance, impact resistance, sufficient hardening depth and uniform surface hardness (Ref 2-4) in order to generate higher rolling force and bear large contact compressive stress and friction.

The alloying element Cr plays an important role in improving the hardenability, wear resistance and carbide precipitation of cold work roll steel. It exists mainly as the M_7C_3 in the steel, which can increase the roll hardness, and reduce the abrasion and waste in the rolling process. A higher amount of hard carbides is also beneficial to the wear resistance of cold work roll (Ref 5). Therefore, the development trend of the cold work roll steel has been mainly dominated by a continuous increase of the alloying element Cr. The steel for cold work roll is based on GCr15

bearing steel in the early stage of rolling machines (Ref 6). After decades of development, the Cr content of the steel increased from 2-5%, in the early days to 8%, 10%, 12% in recent years (Ref 7-8). However, with the rapid development of rolling technology, Cr-series cold work roll steel was not capable of meeting the increased requirement of producing high quality products.

High speed steel (HSS) roll has attracted wide attention in recent years with its higher hardness and red hardness, superior wear resistance and hardenability (Ref 9). The HSS, which belongs to high carbon ledeburitic steel, contains more alloying elements such as W, Mo, Cr, V forming carbides including MC, M_2C , M_6C , M_7C_3 and $M_{23}C_6$ (Ref 10-12). The extremely high hardness (HRC 63-70) can be obtained by special heat treatment, and the hardness and wear resistance can be retained up to 550-600°C (Ref 13). Based on these excellent material properties, HSS rolls have been developed rapidly and applied widely. However, the traditional HSS roll contains more alloying elements W, Mo, which significantly increase the manufacturing cost. In addition, it is necessary that the cold work roll should be forged to produce an optimum balance of strength and toughness, but HSS can not be used to directly make the forged cold work roll due to its tendency to cracking, which has restricted its application over a wider application fields. Development of new steels with optimum properties and formability is essential for this important steel making field.

In this work, a novel steel for cold work roll on the basis of traditional HSS roll was designed and optimized through CALPHAD analysis, in which the W, Mo contents were reduced and Cr content was increased. The new steel not only meets the development trend of cold work roll for high Cr content, but also replaces alloying elements W (Mo) with Cr to achieve higher roll hardness, wear resistance and carbide quantities. The results of the phase diagram and structures established also provide the theoretical basis for design and optimization of the forging process of cold work roll

2. Experimental materials and methods

The specimen was taken from the designed steel for forged cold work roll based on the composition of traditional HSS roll. The chemical composition of the steel is listed in Table 1. The Fe-C isopleths of the steel and the curve of mass fraction of equilibrium phases versus temperature were calculated by Thermo-Calc according to the contents of alloying elements.. Then, the content of a specific alloying element (W, Mo, Cr or V) was changed without variation of other elements, and a new curve of mass fraction of equilibrium phases versus temperature was obtained, from which the mass fraction of austenite, ferrite and all kinds of carbides (MC , M_6C , M_7C_3 , $M_{23}C_6$) were extracted. Subsequently, the curves of mass fraction of a certain phase with different contents of given alloying element were combined, and then the effects of different alloying elements (W, Mo, Cr, V) on austenite, ferrite and all kinds of carbides (MC , M_6C , M_7C_3 , $M_{23}C_6$) were analysed to optimize the designed composition. Finally, the chemical composition for forged cold work roll steel was determined.

The designed and optimized specimens were both quenched at 1100°C and then tempered twice at 560°C. The microstructure of the steel was observed by Axiovert 200 MAT optical microscope (OM) after etched in aqua regia (HNO_3+3HCl). Ten micrographs (200×) were taken for each specimen, and the volume fraction of the carbide was counted by Image-Pro Plus software.

The hardness of specimen was measured under a load of 150 kg by HR-150A Rockwell tester

with a diamond indenter. Five points were obtained on the surfaces of the designed and optimized specimens, and the average value was used to represent the hardness of each specimen. Pin-on-disc tests were carried out on a MMU-10G high temperature tribotester. The pins with dimension of $\Phi 4 \times 15$ mm were machined from designed and optimized steels and employed to abrade on the discs made of 9SiCr steel under an applied load of 100 N at room temperature. The rotational speed of pin was 100 r/min. The run track of pins was circular with a radius of 11mm and the linear speed was kept constant. During each test, the weight loss of the specimen was measured by electronic balance every 30min and averaged over three repeated test results. Hot compressive tests at 1100°C with a strain rate of 1 s^{-1} and 50% deformation was carried out by Gleeble-3500 thermo-simulation machine to simulate the high temperature forging process.

3. Results and analysis

3.1. Phase equilibrium thermodynamic calculation

The initial chemical composition (wt%) of the novel steel for cold work roll is designed as 1.32%C, 11.5%Cr, 3.8% Mo, 2.2% W, 2.8%V, 0.5% Mn and 0.5%Si. The Fe-C isopleths of the steel calculated by Thermo-Calc is shown in Fig.1. The carbon content of the steel is marked by the straight line on the diagram. From Fig.1, ferrite crystallization ($L \rightarrow \alpha$), peritectic reaction, eutectic reaction ($L \rightarrow \gamma + MC$) and precipitation of M_7C_3 , M_6C , $M_{23}C_6$ occur successively, at 1379°C, 1358°C, 1205°C, 1188°C, 1186°C and 952°C respectively.

Fig.2 shows the relationship of mass fraction and temperature of all equilibrium phases. It is clearly shown that the amount of liquid continues to reduce with decreasing temperature and the liquid disappears completely at 1200°C. Austenite (A) crystallizes over a wide temperature range of 850-1350°C. Ferrite (F) precipitates from the liquid at high temperature, followed by peritectic reaction. The peritectic reaction can result in micro-segregation, even macro-segregation, which may reduce the roll performance. Meanwhile, although all carbide contents change with temperature, the total content of carbides is maintained at about 10% to preserve the carbide quantity in subsequent heat treatment in order to meet the requirement of high hardness and wear resistance.

3.2. Effect of alloying element content on mass fraction of all phases

3.2.1. Effect of W content

The curves of mass fraction versus temperature of all phases with increasing W content are shown in Fig. 3. As shown in Fig. 3(a), the effect of W content on the ferrite at low temperature is not significant. However, with increasing W content, the temperature range of peritectic reaction at high temperature increases slightly. From Fig. 3(b), 3(d) and 3(f), the mass fraction of austenite, M_7C_3 and $M_{23}C_6$ exhibits very little change with increasing W content. M_7C_3 and $M_{23}C_6$ are known to be Cr-rich carbides, the result observed demonstrate that the effect of W content on the Cr-rich carbides is small. Evident from Fig. 3(c), the mass fraction of MC decreases when the W content increases, which indicates that W content influences the V-rich carbide. MC disperses in the steel as tiny particles, its stability and hardness are the highest compared to other carbides, so more MC is required in the steel by reducing the W content appropriately. As shown in Fig. 3(e), the effect of W content on M_6C is the most significant one, the reason lies in the fact that M_6C is

a (W, Mo)-rich carbide. With increasing W content, the quantity and precipitation temperature of M_6C increase gradually, and the temperature range widens simultaneously. When W content reaches 0.5-1.0%, M_6C disappears at a temperature range of 850-900°C, which is beneficial for the properties and performance of the steel. The reason is that, with prolonged time, M_6C , formed at higher temperature grows gradually into coarse and irregular blocky carbide, which spalls easily to form internal defect and affects the final mechanical properties of the cold work roll steel. Based these data, W content in the steel is chosen as 0.5-1.0%.

3.2.2. Effect of Mo content

The curves of mass fraction versus temperature of all phases with the increase of Mo content are presented in Fig. 4. It is shown in Fig. 4(a), the effect of Mo content on the ferrite at low temperature is also relatively small, similar to that for element W. With increasing Mo content, the temperature range of peritectic reaction at high temperature increases slightly. From Figs. 4(b), 4(c), 4(d) and 4(f), the effects of Mo content on austenite, V-rich MC, Cr-rich M_7C_3 and $M_{23}C_6$ are not significant. From Fig. 4(e), when Mo content is 2.5-3.0%, M_6C disappears at about 860°C. With further increasing Mo content, M_6C still exists below 800°C, at which point M_6C can coalesce to grow and coarsen resulting in adverse effect on the mechanical property of the roll. In order to lower the cost of cold work roll, W content in this work is expected to be kept below 1%. However, low W content can decrease the roll hardness. The alloying element Mo can play a similar role in the formation of equilibrium phases, phase transformation and mechanical property of the steel as that for element W. Because the relative atomic mass of alloying element Mo, W are 95.94 and 183.9 respectively, the effect of 1%Mo corresponds to that of 2%W, while cost of 1%Mo is merely equivalent to that of 1.2-1.5%W. Therefore, it is economical to replace W by Mo in the steel for cold work roll. In this work, Mo content is not only reduced to narrow the region of the peritectic reaction and precipitated range of M_6C , but also maintains at a certain level to replace alloying element W to ensure the roll hardness. Based on these technical considerations, a Mo content of 2.5-3.0% is considered to be appropriate in this work.

3.2.3. Effect of Cr content

The curves of mass fraction versus temperature of all phases with the increase of Cr content are shown in Fig. 5. From Fig. 5, the variation of Cr content changes the contents of ferrite, austenite and the carbides. Evident from Figs. 5(a), 5(b) and 5(c), with an increase of Cr content, the region of peritectic reaction broadens (When the Cr content is 9%, peritectic reaction disappears), the phase region of austenite becomes narrower and the precipitation amount of MC decreases. As shown in Fig. 5(d), with increasing Cr content, the precipitation region of M_7C_3 broadens and the mass fraction increases in the steel. M_7C_3 is the main carbide in the work layer of cold work roll, the quantity of the carbide affects the wear resistance and hardenability directly. From Fig. 5(e), with increasing Cr content, the mass fraction of M_6C between 950-1200°C increases gradually and then decreases when the temperature is below 950°C. From Fig. 5(f), with increasing Cr content, the mass fraction of Cr-rich $M_{23}C_6$ increases. The tiny and dispersively distributed $M_{23}C_6$ almost fully dissolves into the austenite matrix, which plays an important role on secondary hardening. Based on these factors Cr content 9-10% is determined to be appropriate to ensure good mechanical properties of the cold work roll.

3.2.4. Effect of V content

The curves of mass fraction versus temperature of all phases with increasing V content are shown in Fig. 6. From Fig. 6(a), the effect of V content on ferrite is more significant than that for other elements presented in sections above. With higher V content, the peritectic reaction region is wider at high temperature, with earlier formation of ferrite at low temperature. From Fig. 6(b), a lower V content can widen the austenite region. For example, the corresponding austenite region for 2% V content is nearly 100°C higher than that for 4% V content, which shows that the lower V content has positive effects on the change of austenite. From Fig. 6(c), the effect of V content on MC is the largest. With higher V content, the quantity of MC is higher and the precipitation of MC occurs earlier, which is beneficial to the mechanical property of the cold work roll. As shown in Fig. 6(e), the precipitation temperature of M₆C is about 1185°C with change in V content. At lower temperature, there is very little change in the quantity of M₆C. From Fig. 6(d) and 6(f), the effect of V content on M₇C₃ (Cr-rich carbide) is similar to that of M₂₃C₆ (Cr-rich carbide). The increase of V content can reduce the quantities of M₇C₃ and M₂₃C₆, thus influences the wear resistance, hardness and hardenability of the cold work roll. As discussed above, the roll properties are strongly related to the V content. The designed V content of 2.5-3.0% can satisfy the requirement of precipitation temperature and mass fraction of all phases well. Therefore, the value of V content remains invariant.

3.2.5. Determination of C content

Carbon in high speed steel can combine with alloying elements to form carbides, which influence the overall performance of the steel. The C content in high speed steel is related to the contents of carbide forming elements. The balance carbon equation can be expressed as follow (Ref 14):

$$C_p = 0.033W\% + 0.063Mo\% + 0.060Cr\% + 0.200V\% \quad (1)$$

where C_p is the value of balance carbon. The equation above is based on an assumption that alloying elements W, Mo, Cr, V in the steel combine with carbon to form various carbides such as Fe₄W₂C, Fe₄Mo₂C, Cr₇C₃, Cr₂₃C₆ and VC respectively. C_p can be obtained according to the proportional relationship of carbon and other alloying elements.

The properties of high speed steel is extremely sensitive to C content. With increasing C content, the hardness after tempering i.e. secondary hardening value and red hardness of high speed steel increase, while its toughness decreases gradually. When the C content reaches the C_p value, the highest secondary hardening value can be obtained.

Based on the results and analysis in the above sections (3.2.1-5), the contents of all alloying elements are designed and optimized by Thermo-Calc, in which, W content is 0.5-1.0%, Mo content is 2.5-3.0%, Cr content is 9-10%, and V content is 2.5-3.0%. The value of balance carbon is calculated according to Eq. (1) to be 1.2-1.4%. The C content of the designed steel is within the range of calculated values, which indicates that the C content designed in this work is reasonable. The final optimized chemical composition of the cold work roll steel is listed in Table 2.

3.3. Experimental verification

As detailed in section 3.2, the effects of alloying elements W, Mo, Cr and V on the mass fraction versus temperature curves of ferrite, austenite, MC, M₇C₃, M₆C and M₂₃C₆ in the cold work roll steel were calculated by CALPHAD. The data is used to determine an optimum

chemical composition for the cold work roll steel.. To further investigate the effect of the optimum composition on the improvement of steel roll service life and its formability in forging , the hardness and wear resistance of the optimized cold work roll steel after heat treatment were studied, and the microstructure of the optimized cold work roll steel after forging was analyzed.

3.3.1. Hardness and wear resistance

Fig. 7 shows the hardness of designed and optimized cold work roll steels after quenching and tempering. From Fig. 7, the hardness of the two steels after quenching is higher than that after tempering. Moreover, under the condition of the same heat treatment, the hardness of the optimized steel is higher than that of the designed one. It can also be seen that although the composition of the optimized steel in this work differs from that of the designed one (e.g. with lower level of alloying content), its hardness after tempering is still above 60HRC, which suggests that the optimized composition for cold work roll is reasonable.

Fig. 8 shows the correlation between wear time and weight loss for designed and optimized steel. From Fig. 8, the weight loss of the two steel is approximately proportional to time. After 120mins, the difference of the weight loss between the designed and optimized specimens becomes significantly different. The weight loss of designed steel after 120mins is 27.9mg, while that of optimized one is only 6.2mg. This clearly shows that the wear resistance of the optimized steel has been improved significantly.

3.3.2. Microstructure of the steel after heat-treatments and forging

The designed and optimized steels studied in this work are based on the traditional HSS alloying system for rolls, whose microstructures are known to be ledeburite. Fig. 9(a) shows a typical ledeburite microstructure of optimized steel after a heat-treatment scheme of quenching+tempering. It is clearly shown that a large number of carbides distribute along the grain boundary forming a carbide network. From the micrograph at higher magnification, it can be observed that the carbides at the grain boundary mainly consist of fibrous M_7C_3 and blocky MC. The determination of carbide types and corresponding carbide morphologies have been investigated in detail in previous work of the authors (Ref 15). Fig. 9(b) shows a typical microstructure of the optimized steel forged at 1100°C. Full field observation showed that No crack was observed on the surface of the forged specimen. The carbide network has also disappeared breaking into large quantities of tiny blocky carbides dispersed in the matrix, these hard particles would give the steel a higher hardness and wear resistance and effectively prevent cracking during the forging and heat-treatment process.

4. Discussion

It is known that M_7C_3 is a Cr-rich carbide. From Fig. 5(d), Cr content mainly influences the mass fraction of M_7C_3 . In this study, Cr content reaches above 10%wt in both of the designed and optimized steels, so M_7C_3 distributes along the grain boundary predominantly, this is evident in Fig. 9(a). Simultaneously, a certain amount of MC is observed at the grain boundary. MC is rich in V, and V content is just lower than Cr content in the two steels. From Fe-C isopleths (Fig. 1), M_6C , a W/Mo-rich carbide, precipitates during solidification. While W and Mo content in the designed steel are lower compared with traditional HSS. After optimization, their contents decrease further, so the typical fishbone-like M_6C observed in HSS, is rarely observed in the

optimized steel. $M_{23}C_6$ is also a Cr-rich carbide and predicted to precipitate at 952°C , but it is not observed in Fig. 9(a) either. This is due to the fact that $M_{23}C_6$ distributes dispersedly in the matrix as small particles with $0.3\text{--}0.5\mu\text{m}$ in diameter. When the specimens are compressed in forging, the carbides break into small fragments and distributes uniformly in the matrix, which can improve the mechanical properties significantly.

Table 3 lists the volume fraction of carbides in the designed and optimized steels after quenching and tempering. It is clearly shown that the volume fraction of the carbides increases after tempering in these two steels, which is caused by the precipitation of the secondary carbides during tempering. It also can be seen that the volume fraction of the carbides in the optimized steel is a little lower than that in the designed one with the same heat treatment. This is because that the contents of carbide forming elements, i.e. Cr, Mo and W, in the optimized steel are lower than that in the designed one, which result in the decrease of the volume fraction of the carbides. However, from Fig. 7 and Fig. 8, the hardness and wear resistance of the optimized steel with less carbides are much better than the designed one, which demonstrates a clear improvement in both composition and properties in the optimized steel based on based on ALPHAD analysis.

5. Conclusion

A novel steel with high Cr and low W, Mo for forged cold work roll was designed and analysed based on the composition of HSS roll. The phase structure of ferrite crystallization, peritectic reaction, austenite crystallization and the precipitation of MC, M_6C , M_7C_3 , $M_{23}C_6$ during equilibrium solidification process was established based on according to Thermo–Calc. The effects of the alloying elements are systematically studied. The elements W and Mo mainly affect the precipitation of M_6C , while Cr affects the precipitated region and mass fraction of M_7C_3 . Higher V content widens the high temperature region of the peritectic reaction, and a large amount of MC precipitates. The optimized composition for cold work roll steel is 1.30–1.35% C, 9–10% Cr, 2.5–3.0% Mo, 0.5–1.0% W, 2.5–3.0% V, 0.5–0.6% Mn, 0.5–0.6% Si. With a quenching and tempering heat-treatment scheme, the hardness reached 60.8HRC and weight loss after 120min is 6.2mg, which meets the high service requirement of hardness and wear resistance for cold work roll. Detailed microstructural study showed that the ledeburite in the optimized steel disappears after forging and the carbide network breaks into a large amount of tiny blocky carbides dispersed on the matrix without cracks demonstrating a good formability in forging of the steel and rationality of the optimized composition.

References

1. A.K. Ray, K.K. Mishra, G. Das, and P.N. Chaudhary, Life of Rolls in a Cold Rolling Mill in a Steel Plant – Operation Versus Manufacture, *Eng. Fail. Anal.*, 2000, **7**, p 55–67
2. H.C. Li, Z.Y. Jiang, A.K. Tieu, W.H. Sun, and D.B. Wei, Experimental Study on Wear and Friction of Work Roll Material with 4%Cr and added Ti in Cold Rolling, *Wear*, 2011, **271**, p 2500–2511
3. P. Montmitonnet, Hot and Cold Strip Rolling Processes, *Comput. Method Appl. Mech. Eng.*, 2006, **195**, p 6604–6625
4. C.R.F. Azevedo, and N.J. Belotti, Failure Analysis of Forged and Induction Hardened Steel Cold Work Rolls, *Eng. Fail. Anal.*, 2004, **11**, p 951–966
5. S. Iwadoh, and T. Mori, Effect of Work Roll Materials and Progress of Manufacturing Technology on Cold Rolling and Future Developments in Japan, *ISIJ Int.*, 1992, **32**, p 1131–1140

6. S. Wang, and D.Q. Liu, Development of the Steel for Forged Cold Work Roll, *Metal Forming*, 2013, **5**, p 70–72 (in Chinese)
7. G. Wang, X. Liu, and J. Wang, Roll and Technique Coolant Lubrication for Cold Tandem Rolling, *Steel Roll.*, 2003, **6**, p 42–46
8. S. Shimizu, K. Aoki, M. Kobayashi, T. Saito, Y. Yamada, and F. Kosumi, A Ti-enhanced Cold Rolling Work Roll with Self-generating Optimal Roughness Characteristics, *ISIJ Int.*, 1992, **32**, p 1238–1243
9. V. Vitry, S. Nardone, J.-P. Breyer, M. Sinnaeve, and F. Delaunois, Microstructure of Two Centrifugal Cast High Speed Steels for Hot Strip Mills applications , *Mater. Des.*, 2012, **34**, p 372–378
10. K.C. Hwang, S. Lee, and H.C. Lee, Effects of Alloying Elements on Microstructure and Fracture Properties of Cast High Speed Steel Rolls. Part I: Microstructure Analysis, *Mater. Sci. Eng. A*, 1998, **254**, p 282-295
11. X.D. Zhang, W. Liu, D.L. Sun, and Y.G. Li, The Transformation of Carbides during Austenization and Its Effect on the Wear Resistance of High Speed Steel Rolls, *Metall. Mater. Trans. A*, 2007, **38**, p 499-505
12. S.Z. Wei, J.H. Zhu, L.J. Xu, and R. Long, Effects of Carbon on Microstructures and Properties of High Vanadium High-speed Steel, *Mater. Des.*, 2006, **27**, p 58-63
13. H.G. Fu, Y.H. Qu, J.D. Xing, X.H. Zhi, Z.Q. Jiang, M.W. Li, and Y. Zhang, Investigations on Heat Treatment of a High-speed Steel Roll, *J. Mater. Eng. Perform.*, 2008, **17**, p 535-542
14. Y.K. Deng, J.R. Chen, and S.Z. Wang, *High Speed Tool Steels*, The Metallurgical Industry Press, Beijing, 2002
15. J. Guo, L.G. Liu, Q. Li, Y.L. Sun, Y.K. Gao, X.J. Ren, and Q.X. Yang, Characterization on Carbide of a Novel Steel for Cold Work Roll During Solidification Process, *Mater. Charact.*, 2013, **79**, p 100-109

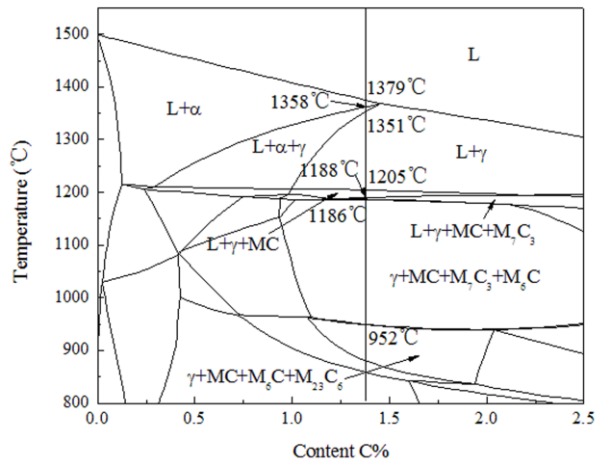


Fig.1. Fe-C isopleths of the steel for cold work roll.

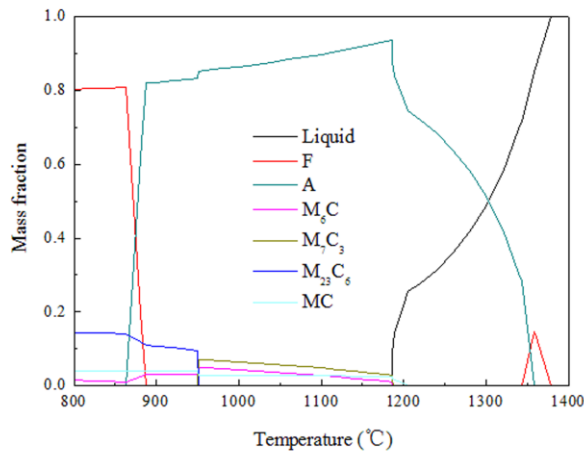


Fig.2. Mass fraction-temperature curve of equilibrium phases for cold work roll steel.

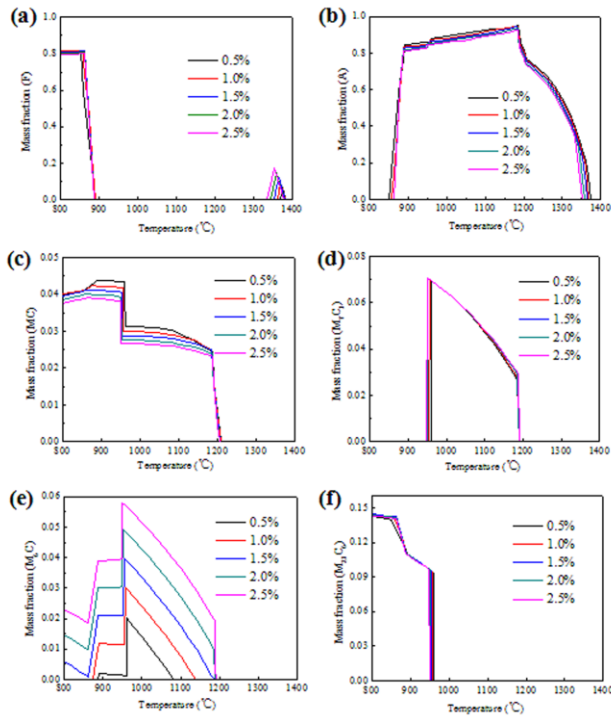


Fig.3. Effect of W content on all phases: (a) F, (b) A, (c) MC, (d) M_7C_3 , (e) M_6C and (f) $M_{23}C_6$.

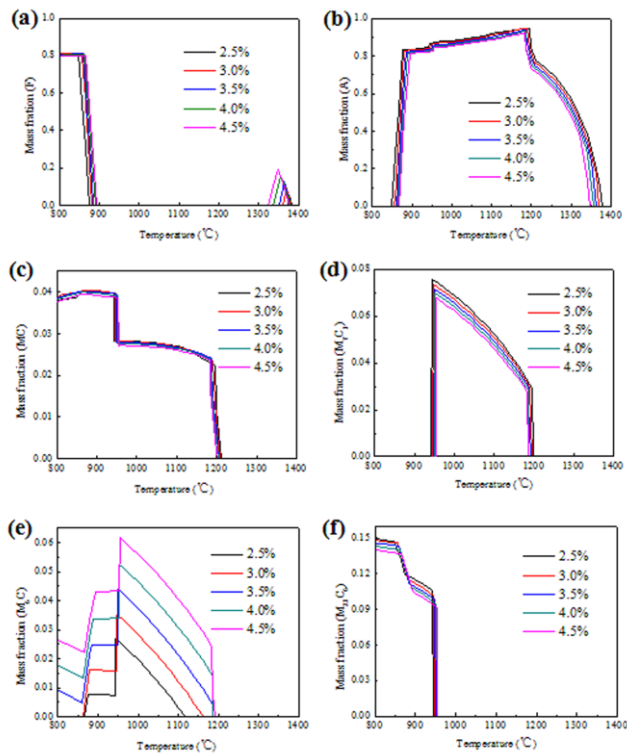


Fig.4. Effect of Mo content on all phases: (a) F, (b) A, (c) MC, (d) M_7C_3 , (e) M_6C and (f) $M_{23}C_6$.

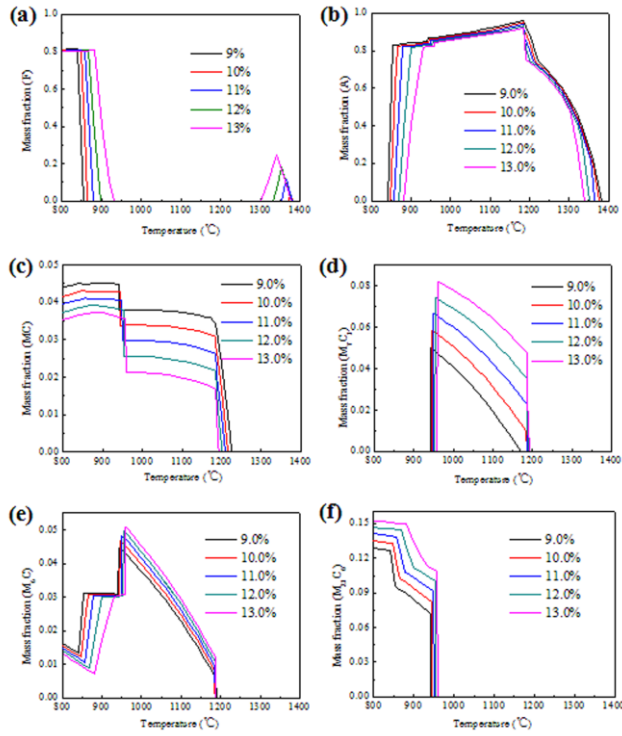


Fig.5. Effect of Cr content on all phases: (a) F, (b) A, (c) MC, (d) M_7C_3 , (e) M_6C and (f) $M_{23}C_6$.

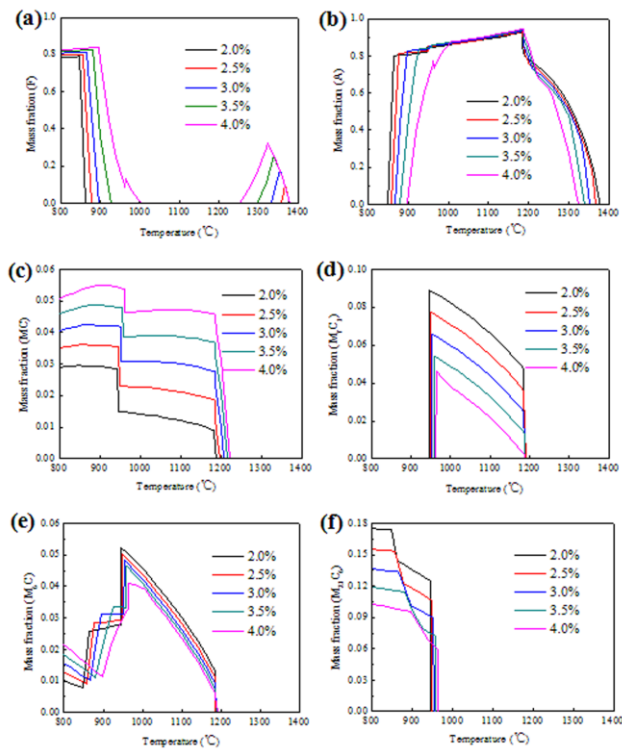


Fig.6. Effect of V content on all phases: (a) F, (b) A, (c) MC, (d) M_7C_3 , (e) M_6C and (f) $M_{23}C_6$.

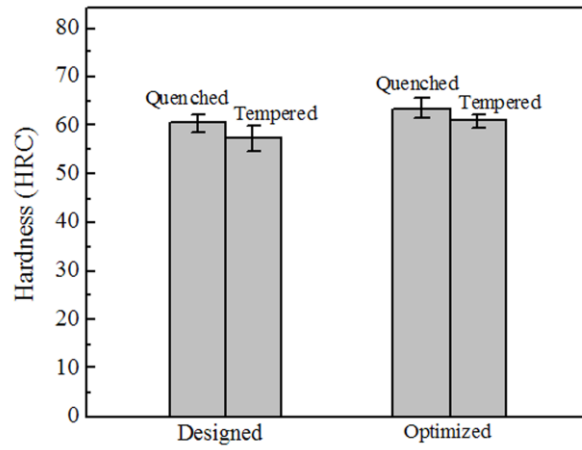


Fig.7. Hardness of the designed and optimized steels after quenching and tempering.

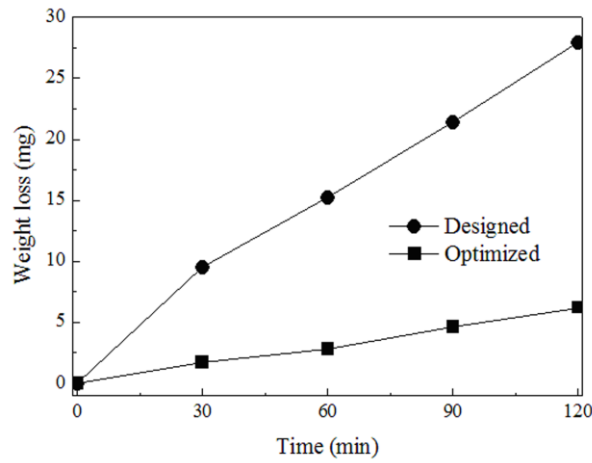


Fig.8. Correlation between wear time and weight loss for designed and optimized steels.

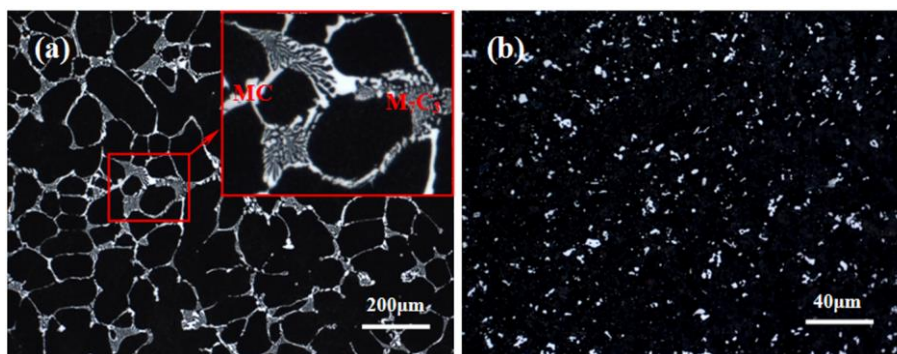


Fig.9. Microstructures of the optimized steel after tempering and forging.

Table 1 Designed chemical composition of the steel for cold work roll (wt. %)

Element	C	Cr	Mo	W	V	Mn	Si	Fe
Content	1.30-1.35	11-12	3.6-4.0	2.0-2.5	2.5-3.0	0.5-0.6	0.5-0.6	Bal.

Table 2 Optimized chemical composition of the steel for cold work roll (wt. %)

Element	C	Cr	Mo	W	V	Mn	Si	Fe
Content	1.30-1.35	9-10	2.5-3.0	0.5-1	2.5-3.0	0.5-0.6	0.5-0.6	Bal.

Table 3 Volume fraction (%) of the carbide in the designed and optimized specimens

Samples	Quenched	Tempered
Designed composition	9.87	12.09
Optimized composition	8.55	10.16